PERFORMANCE INSIGHTS FROM AMBIENT VIBRATIONS: UNVEILING THE DYNAMIC INTERPLAY OF STRUCTURES IN A LARGE DAM

Michael Dupuis, PE, PEng, MASc[1], Brian Martinez, PhD[1], Tom MacDougall, PE[2], Josh Corbett, PE[3]

(Part 2 of a three-part paper series)

ABSTRACT

Ambient vibration data acquired from 90 unique locations on a large dam were evaluated to investigate the dynamic behavior and system interactions of its structural components. This data collection program was designed to validate the dynamic properties of an LS-DYNA model, which is being used to evaluate the dam's response to earthquake ground motions. Results of the dynamic structural analysis will be used to inform an ongoing Issue Evaluation Study by the U.S. Army Corps of Engineers. Ambient vibration data were recorded over four days during normal operating conditions without forced excitation of the structure. Eleven recording instruments—four reference instruments and seven temporary instruments—were deployed for thirteen 40-minute-long test setups. These setups included locations along the right and left embankment roadways, within the three galleries (right retaining wall, lower gallery, and upper gallery), on various parts of all five spillway piers (trunnion anchor blocks, upper landing, and pier top), within the penstock hoist motor room, and at various elevations of the elevator tower. The ambient responses were evaluated based on their spectral content and power spectral densities were used to identify where dominant behavior occurs in the dam and its components. Interaction effects were identified by comparing resonances within the dam that manifested as split resonances, indicating coupling between the components. A systems approach was used to describe the results for the entire dam and how the individual components interact. Estimates of damping showed the greatest damping in the portions of the concrete dam adjacent to the embankments and the lowest damping at the interior piers. The results of the various analysis methods indicate that the dam is a highly coupled complex system with significant interactions between various components, which are expected to influence the seismic response of the structure.

INTRODUCTION

The Risk Management Center (RMC) of the United States Army Corps of Engineers (USACE) is conducting Issue Evaluation Studies (IES) on multiple dams in the Willamette River Valley, located in Oregon. One of the primary components of these studies is to better characterize the potential seismic risk by conducting detailed structural analyses of the dams considering static and seismic loading. As part of these assessments, linear and nonlinear finite element models with both frequency- and time-domain analyses in LS-DYNA, an advanced general-purpose multi-physics simulation software,

[1] Geosyntec Consultants Inc.
[2] RJH Consultants Inc.
[3] United States Army Corps of Engineers

are being used to better understand the seismic performance of dams within the USACE IES process. Foster Dam, a rockfill earthen embankment dam with a central concrete spillway, is the first such analysis currently underway.

For certain potential failure modes of Foster Dam, the structural demands, failure thresholds, and potential damage may be sensitive to the dynamic characteristics of the structural model, in particular the modal frequencies, damping, and interactions between the various structural components. Therefore, validation and calibration of the dynamic properties in the finite element model with recorded data are necessary.

Ambient vibration data were recorded from various critical components of Foster Dam, labelled in Figure 1, which included the concrete gravity monoliths, a reinforced concrete tower, spillway piers, and adjacent embankments, including the spillway retaining walls. The ambient vibration data were analyzed to identify the dynamic characteristics of various features of the dam in support of development of finite element models and to improve understanding of the system interactions of the structural components.

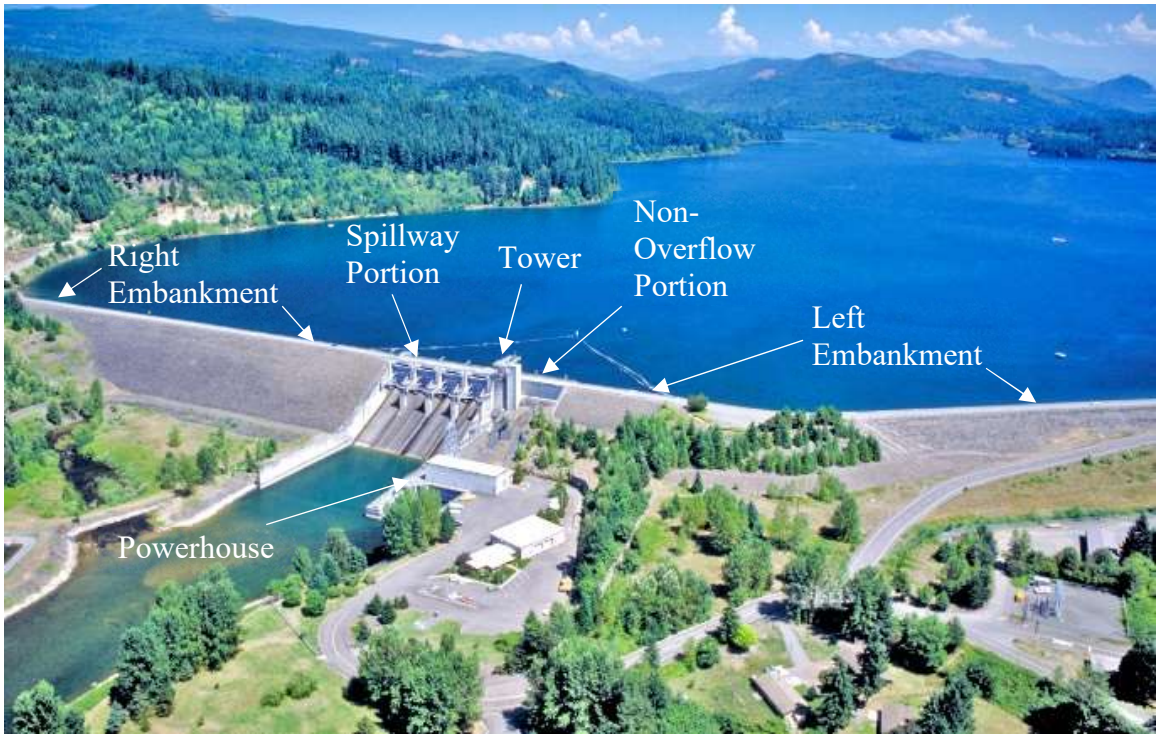

Figure 1. Aerial view of Foster Dam looking upstream (Recreation, 2024).

DATA SUMMARY AND BACKGROUND

Ambient responses were acquired using accelerometers with 2-g full scale range and with self-noise of 20 $\mu g/\sqrt{Hz}$ (Sensequake, 2023) and velocimeters with 120 mm/s full-scale range and with 10^{-2} $\mu g/\sqrt{Hz}$ self-noise from 1 to 20 Hz (Sensequake, 2023). Data quality was assessed based on a review of the time and spectral characteristics. The recorded vibrations include both steady-state ambient noise and transient events. Transient events

which were essentially uncontrolled forced excitations, were caused by vehicles passing over the road along the crest of the dam.

To facilitate different methods of analysis, which can variously make use of steady-state and transient data, windows of each type of behavior were extracted from each test setup and stand-alone deployment, as shown in Table 5 for Test Setup-3 (TS-3). The acceleration data is judged to be best suited for the relatively high-amplitude transient events, which exhibit up to 0.2 g during the arrival of vehicle-induced transients. The velocity data is judged to be best suited for steady-state recordings (i.e., data recorded during the road closure) for which ambient acceleration levels range from 1 to 5 mg.

For test setups recorded while the crest road was open, transient events, such as those apparent in Figure 2, were introduced by vehicles as they moved longitudinally along the axis of the dam; therefore, the timing of the peak accelerations differs at different instrument locations. A trimmed duration of 15 seconds was found to be sufficient to encompass transient vibrations at all sensors for each event. Seven transient events were selected from each test setup and stand-alone deployment. Instances where multiple vehicles caused closely spaced transients, visible in the time domain as overlapping wave trains, were not selected.

TS-8, TS-9, TS-10, TS-A, and Stand Alone Deployment (SAD) -Bedrock (refer to part 1 for dam feature and instrument locations) did not contain transient events because they were recorded while the crest roadway was closed or were recorded from downstream bedrock well separated from the roadway. Low-amplitude steady-state ambient vibrations along the right embankment during TS-8 are shown in Figure 3. However, for some of these recordings, there was still some slight variation of background noise, which was possibly introduced by foot traffic or operation of the elevator; therefore, preferred windows of true steady-state data are provided in Table 5 which do not necessarily encompass the entire record duration.

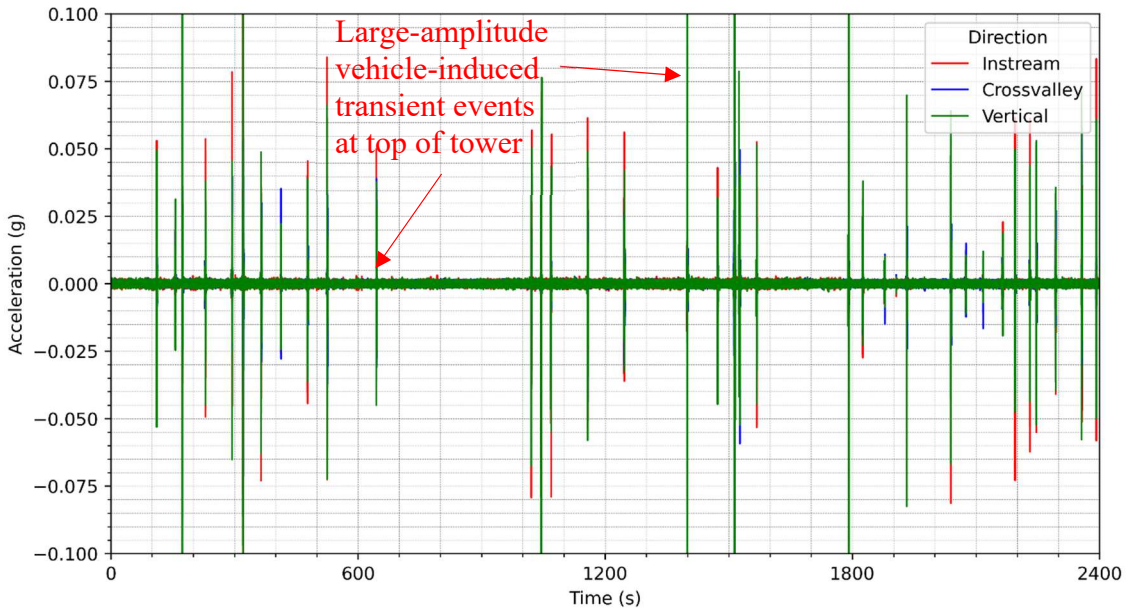

Figure 2. Ambient response acceleration time series data collected from Tower — Top Level (TS-6, Instrument 1) while the crest road was open.

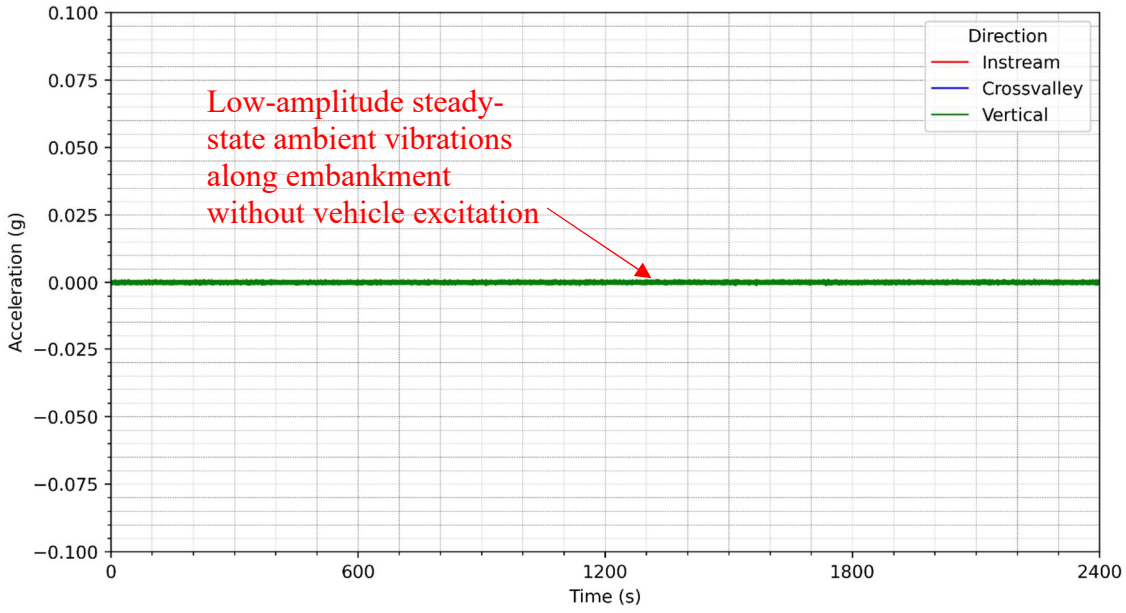

Figure 3. Ambient response acceleration time series data collected from the Right Embankment — Station 21+70.0 (TS-8, Instrument 4) during the crest road closure.

DATA PRE-PROCESSING

The following pre-processing steps were applied to all full-length recorded time series. These processing steps were applied to both the acceleration recordings, and the velocity recordings from each instrument:

1. Load either acceleration data (for transient events) or velocity data (for steady-states) from the human-readable text files. For velocity data, the derivative of the signal was computed to convert from units of velocity to acceleration;
2. Scaled records from units of m/s^2 to g;
3. The 15-s time series for each transient event was trimmed and extracted as an independent time series, as shown in Figure 4. Similarly, the steady-state portions were segmented into 15-s-long time series and were extracted as independent time series;
4. Linear detrend and removal of mean offset for each segmented time series;
5. The segmented 15-s-long time series were set to have start times of 0 s;
6. A Tukey (tapered cosine) window was applied to each segmented time series with 10% of the duration within each tapered region at the start and end; and
7. Rotation of the horizontal components to be orthogonal with the longitudinal and transverse axis of the dam (as required).

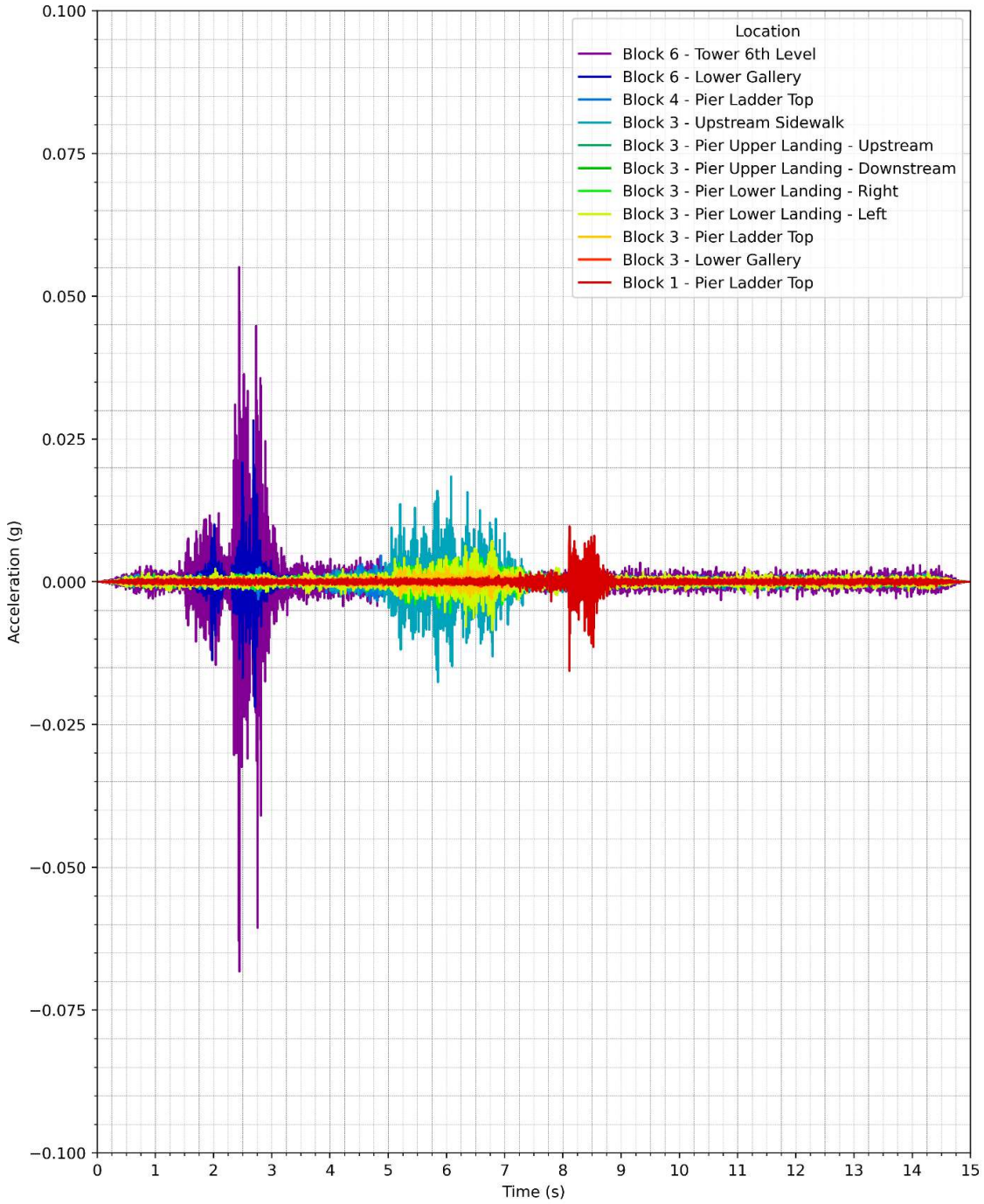

Figure 4. Pre-processed vertical acceleration time series for all instruments for Test Setup 3 for the transient event from 775 s to 790 s.

POWERHOUSE HARMONICS

A stand-alone deployment with a single instrument was used to record data from bedrock from an accessible location adjacent to the powerhouse and downstream of the left embankment approximately 230 ft from the powerhouse turbines. These data were investigated to identify the presence of harmonics associated with rotating equipment from the powerhouse. Large peaks in the fast Fourier transformation (FFT)-based power spectral density (PSD) in all three directions were found to be present at multiples of 4.285 Hz, as shown in Figure 5. These harmonics are suspected to be associated with the frequency of rotating machinery within the powerhouse. By identifying the powerhouse harmonics from the bedrock location, which was relatively isolated from the structural components of the dam, there can be greater confidence that peaks at identical frequencies observed in spectra from other structural components are due to influences of these harmonic vibrations. These suspected powerhouse harmonic frequencies are indicated in all spectral plots as vertical dashed lines.

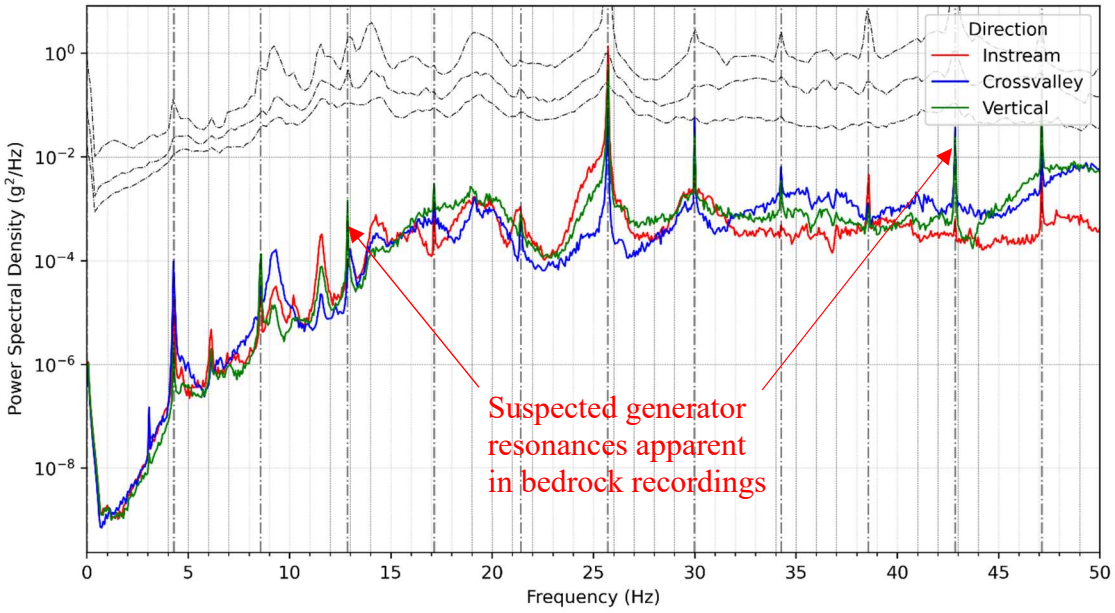

Figure 5. Bedrock power spectral densities with suspected harmonic frequencies emanating from the powerhouse apparent as spectral peaks at multiples of 4.285 Hz. The instream and crossvalley channels were slightly skewed; however, the skew angles were not recorded.

The rigid formulation of the FFT-based PSD includes amplitudes of the complex exponential that exactly reproduces the signal and noise. This results in high variability in amplitudes over relatively small changes in frequencies and makes it difficult to identify the powerful resonant behavior with which we are concerned. Therefore, PSD computed via entropy-based methods, which better account for the dominant energy of the system, are considered in the subsequent sections.

IDENTIFICATION OF STRUCTURAL RESONANCES

To address these shortcomings in the FFT-based spectra, an entropy-based technique—the Maximum Entropy Method (MEM)—was adopted for estimating PSD, and MEM-based PSD were used to identify frequencies in the structures that contain the most power. MEM-based PSD remove the rigid mathematical constrictions of periodicity and instead rely on curve fitting to the power of the signal based on the contents of the signal (Marple, 1987). It is noted that spectral peak widths of the power spectral densities computed via the maximum entropy method are sensitive to the selected model order and therefore judgement was required to determine appropriate parameters.

Horizontal-to-vertical spectral ratios (HVSR), and various geomean spectra thereof, were computed for each pre-processed time series. The following procedure, which is similar to that of Smith et al (2024) who analyzed earthquake-induced records at embankment dams, was applied to compute HVSR at various locations on different structural components of the concrete portion of the dam:

1. Load the pre-processed acceleration time series from .aaa format;
2. Calculate the MEM-based PSD for each channel of each segmented transient event;
3. Calculate the horizontal-to-vertical spectral ratio, for both the instream horizontal and crossvalley horizontal directions, by dividing the PSD for each horizontal channel by the corresponding PSD for the vertical channel;
4. Compute the square root of these PSD ratios; and
5. Calculate the geomean of the HVSR computed for each instrument location.

These HVSR provided insights into resonant behavior in various structural components. Example HVSR plots for two portions of the dam—the concrete non-overflow and along the right embankment—are shown in Figure 6 and Figure 7. For reference locations, or temporary locations that were part of multiple test setups, multiple lines are shown—one for each test setup.

The instream HVSR for the concrete non-overflow portion of the dam (Figure 6) indicates instream resonances for the tower, visible as peaks at approximately 13.5 Hz. For locations within the concrete monolith, there are no distinct resonant. A large trough at 25.7 Hz corresponds to a high-energy powerhouse harmonic apparent for all instruments in this portion, regardless of location in the structure.

The instream HVSR for the right embankment (Figure 7) indicates significant peaks between 3.5–11.5 Hz. For stations between 1860 and 2170 ft, which are located along the right embankment in regions where it has its maximum height, the spectral peaks occur at approximately 3.5 Hz. For stations that are further crossvalley right, the embankment height at these locations progressively decreases, and this appears to be reflected in the dominant instream resonances detected at these locations 5 Hz (Station 17+05.0), 8.5 Hz (Station 15+50.0), 9.5 Hz (Station 13+95.0), and 11.5 Hz (Station 12+40.0).

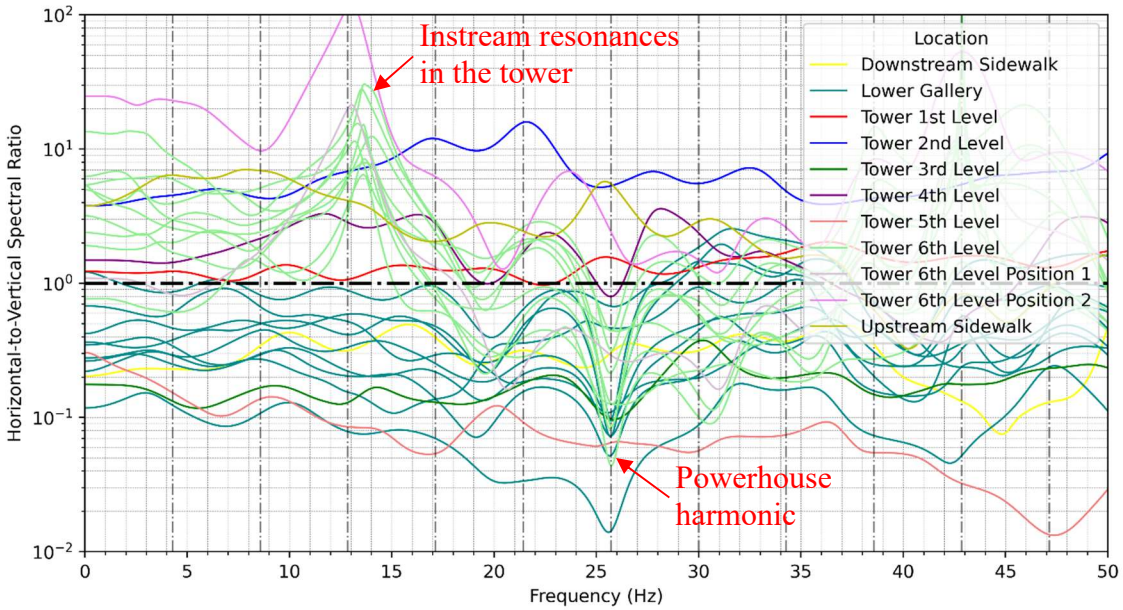

Figure 6. Block 6 — instream horizontal-to-vertical spectral ratio (all test setups with transient events and SAD-Tower).

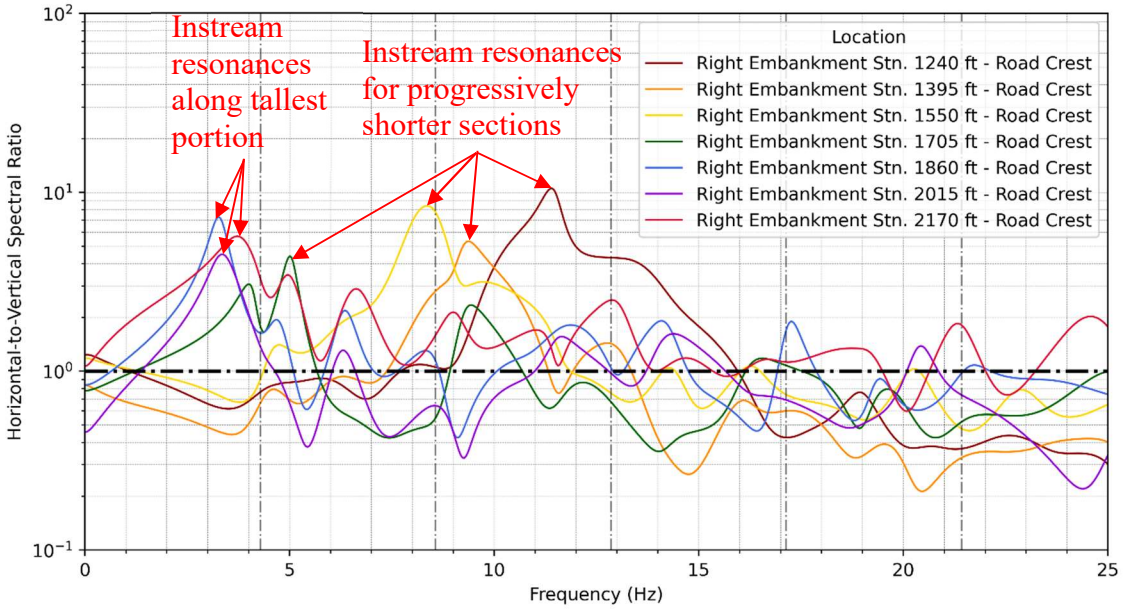

Figure 7. Right embankment roadway crest — instream horizontal-to-vertical spectral ratio (TS-8).

IMPORTANT COMPONENT INTERACTIONS

The following procedure was applied to compute structure-to-gallery spectral ratios (SGSR) at various cross-sections for selected structural components of the dam. A single gallery location was used for each block—the gallery location within that block. Eight gallery locations were used in total, one for each concrete dam block. For Block 1 through Block 5, these were located within the lower gallery; for Block 6 through Block 8, these were located within the upper gallery. The following processing steps were applied to the pre-processed time series to compute the SGSR at all locations in the concrete portion of the dam.

1. Load the pre-processed acceleration time series from .aaa format;
2. Calculate the MEM-based PSD for each channel of each segmented transient event;
3. Calculate the SGSR by dividing the PSD for each transient event's structural channel by the corresponding PSD for each gallery channel (e.g., instream structural channels were compared to instream gallery channels within each cross-section);
4. Compute the square root of these PSD ratios; and
5. Calculate the geomean of the SGSR for each instrument of each test setup.

Significant crossvalley interaction effects are observed for the piers and the tower, as shown in Figure 8 and Figure 9, for the Block 2 pier and the Block 6 tower, respectively. Because the resonances of the various components interact and compete (interacting components cannot share a common frequency), the resonant peaks for the piers in the crossvalley direction are slightly offset but occupy frequencies from 10–14 Hz. There is a corresponding dead zone—a frequency band with attenuated behavior—in the tower crossvalley direction from 10–14 Hz, which is evident from the slight trough in the range. These interaction effects were observed during the low-level ambient vibrations of the testing program and would be expected to increase with stronger shaking (i.e., at ambient levels, the interaction effects may not be fully developed).

Estimates of resonant frequencies for various structural components of interest were made. These estimates are summarized and presented for the concrete spillway and non-overflow portion in Table 1. The interaction effects may indicate that there are relatively competent interfaces between the structural components (piers and tower). However, during very strong ground shaking, i.e., the conditions with which we are primarily interested, these interfaces may degrade or separate, at which point the interaction effects would diminish, the attenuated behavior observed in the tower may decrease, and the crossvalley resonances in the piers may shift as they no longer compete to occupy the same spectral frequencies.

Table 1. Approximate resonant frequency estimates, in Hz, for each structural component of the concrete spillway and non-overflow portion. Approximate resonances are indicated, observed peaks varied approximately +/- 1 Hz between instruments and test setups. Approximate maximum heights, measured from bedrock shown in Appendix A, are provided in parentheses.

Structural Component	Instream Mode	Crossvalley Mode
Pier 1 (Right Retaining Wall) (115 ft)	-	9.5 Hz
Pier 2 (110 ft)	15 Hz	12 Hz
Pier 3 (85 ft)	16 Hz	14 Hz
Pier 4 (85 ft)	15 Hz	12 Hz
Pier 5 (90 ft)	13.5 Hz	19.5 Hz
Tower (105 ft)	13 Hz	11.5 Hz

In a parallel analysis to the spectrum-based analysis, ARTeMIS Modal (ARTeMIS, 2023) was used to complete an operational modal analysis (OMA). OMA is a powerful technique which can be used to determine deflected mode shapes from ambient vibration data. Mode frequencies and shapes estimated via the frequency domain decomposition (FDD), enhanced frequency domain decomposition (EFDD), and curve-fit frequency domain decomposition (CFDD) methods. The three methods were found to produce very similar estimates of frequencies and deflected mode shapes.

EFDD was used to produce the frequency and mode shapes shown in Figure 10 and Figure 11 for the spillway portion of the concrete dam. ARTeMIS relies on the singular value decomposition, therefore, for the global model shown in Figure 10 and Figure 11, local resonances which were identified at similar but adjacent frequencies by spectral-based methods, were combined into a single global mode and frequency.

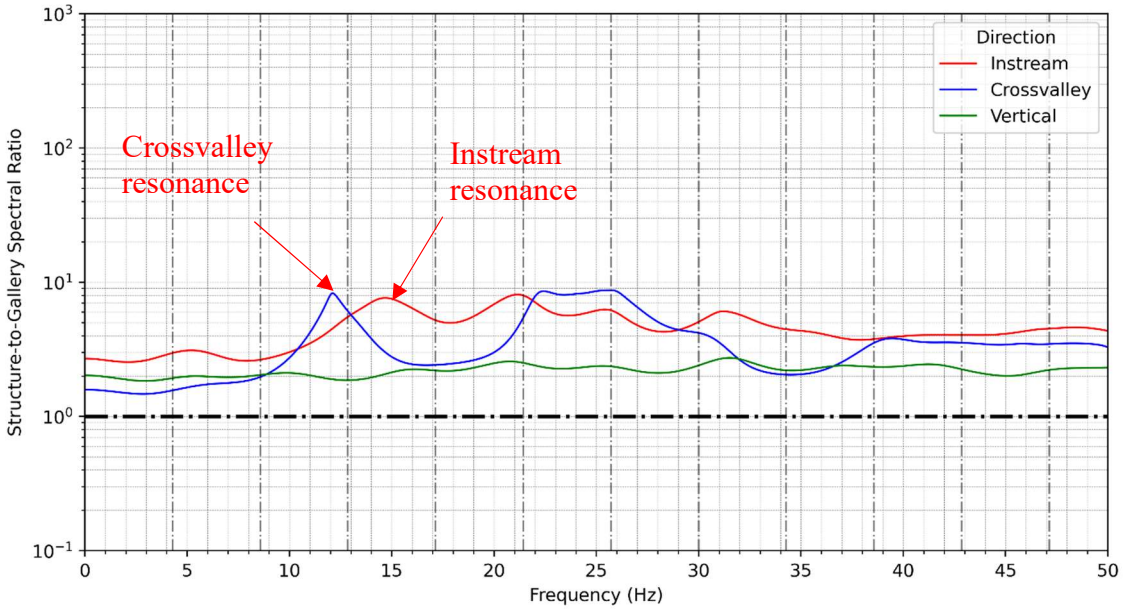

Figure 8. Block 2 — Pier Ladder Top structure-to-gallery spectral ratio (TS-2).

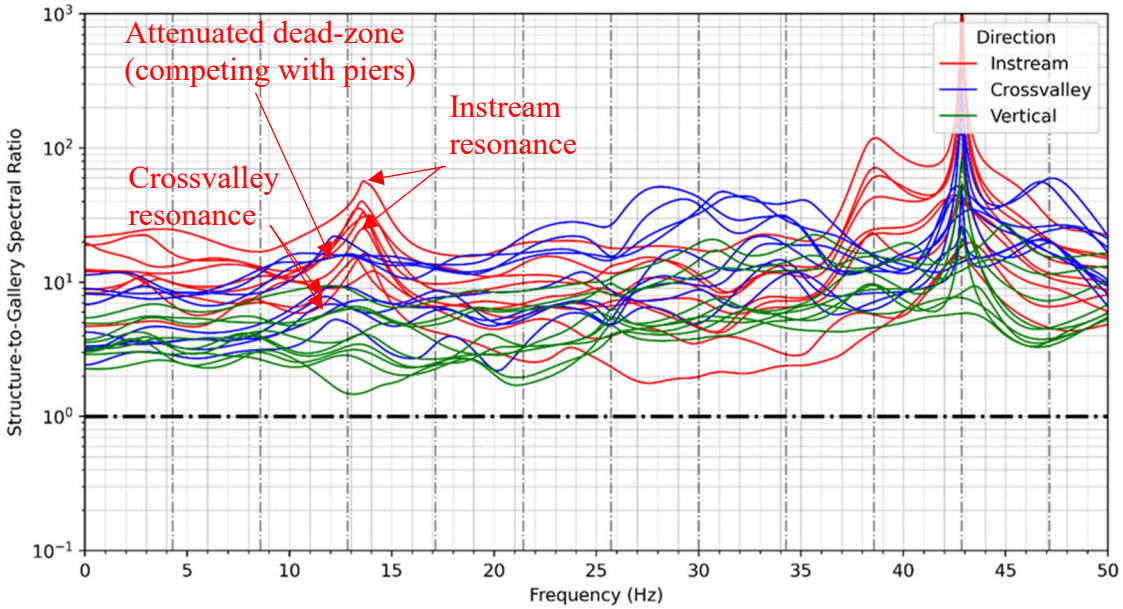

Figure 9. Block 6 — Elevator Tower — 6th Level (top level) structure-to-gallery spectral ratio (all test setups with transient events).

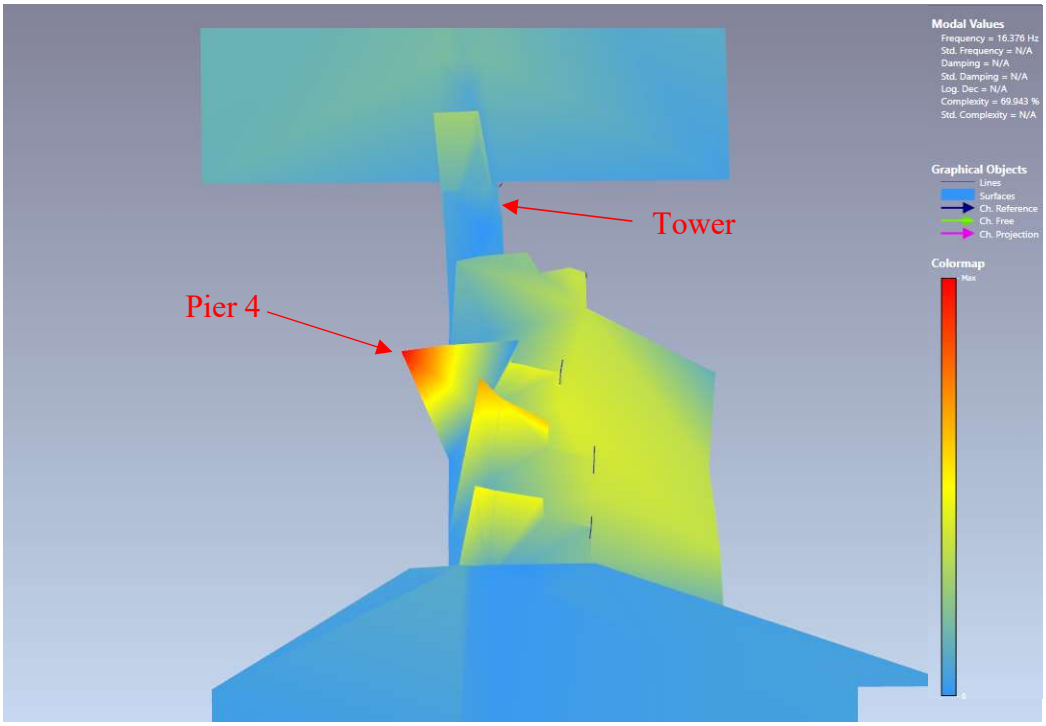

Figure 10. Deflected global instream mode shape estimated at 16 Hz (ARTeMIS, 2023).

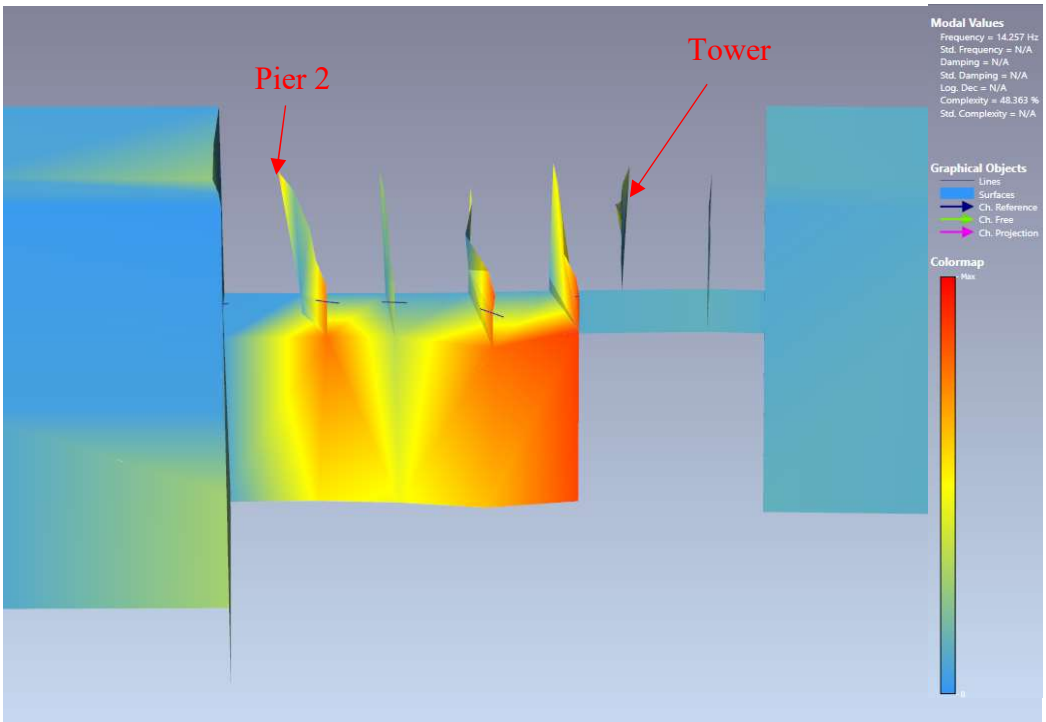

Figure 11. Deflected global crossvalley mode shape estimated at 14 Hz (ARTeMIS, 2023).

IMPLICATIONS FOR SEISMIC RESPONSE

The results of the various analysis methods indicate that Foster Dam is a highly coupled complex system with important interactions between the various components. Important resonant behavior, which is expected to drive the seismic response of the structure and various structural components, was identified. The dynamic behaviors observed are representative of low-amplitude structural response conditions and are likely to strengthen as stronger shaking fully activates the interactions and then significantly change if very intense shaking degrades the coupling effects between components through structural damage.

CONCLUSION

Ambient vibration data acquired on Foster Dam were evaluated to elucidate the dynamic behavior and system interactions of the structural components. The data were recorded over four days during close to normal operating conditions and without forced excitation of the structure. Eleven recording instruments (four reference instruments and seven temporary instruments) were deployed for thirteen 40-minute-long test setups. The 13 test setups included locations along the right and left embankment roadway, within the three galleries (right retaining wall, lower gallery, and upper gallery), on various portions of all five spillway piers (trunnion anchor blocks, upper landing, and pier top), within the penstock hoist motor room, and at various elevations up the height of the elevator tower. An additional standalone recording was made on bedrock to identify powerhouse harmonics.

The ambient responses were evaluated based on their spectral content with power spectral densities used to develop an understanding of where dominant behavior exists in the dam and its components. Interaction effects were identified by comparing resonances within the dam that manifested as split resonances—apparent as adjacent peaks separated by a slightly dipping plateau—which indicates tuned vibration absorption from an adjacent component. The analysis indicates that Foster Dam is a complex system with significant interaction between the various structural subcomponents. Specifically, the tower and the piers exhibit interactions that produce regions of attenuated and shifted behaviors in both components. This is significant because shifted and depressed responses can be expected in each region while the interaction effects persist; however, this damping effect would end should the structures become isolated due to damage during significant ground shaking.

The results of the various analysis methods indicate that Foster Dam is a highly coupled and complex system with important interactions between the various components. Important modal behavior, which is expected to drive the seismic response of the structure and various structural components, were identified. The results presented herein are representative of low-amplitude structural response conditions. In general, the interaction effects will progressively increase as shaking intensity and duration increases, until the severity of earthquake-induced shaking becomes so intense that the interfaces between the various components degrades, and the components transition to behave as individual structures.

This paper is part 2 of a series of technical papers on ambient vibration data collection (part 1), component interactions (part 2), and LS-DYNA modeling effort (part 3). Future studies will apply the estimated dynamic properties and important component interactions affecting the seismic response, determined from the ambient vibration testing to validate an LS-DYNA model of Foster Dam.

ACKNOWLEDGEMENTS

The authors would like to thank the Risk Management Center of the U.S. Army Corps of Engineers for supporting this initiative and granting permission to publish this paper. The authors also wish to thank Larry Nuss and Osmar Penner for serving as external reviewers.

REFERENCES

ARTeMIS Modal (2023). https://svibs.com/.

Marple Jr, S. L. (1987). Digital spectral analysis with applications. Englewood Cliffs.

Sensequake (2023). https://www.sensequake.com/

Smith, J. F., Ball, J. S., Novoa, N., Meremonte, M., & Levish, D. (2024). One station to rule them all: Can one seismic station forecast seismic performance of embankment dams? Paper presented at the United States Society on Dams Conference, April 17-21, Seattle, WA.